Analyst

Accepted Manuscript

ROYAL SOCIETY OF CHEMISTRY

www.rsc.org/analyst

Graphic abstract:

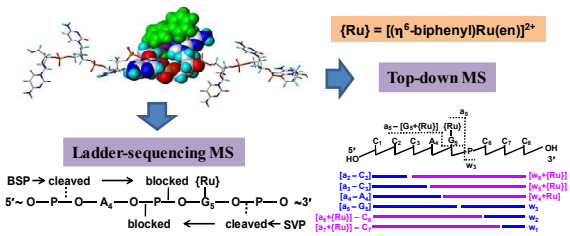

Top-down MS analysis provided sequential and complementary fragments, being more efficient than ladder-sequencing MS to discriminate binding sites of a ruthenium anticancer complex bearing a bulky ligand to oligonucleotides.

Journal Name

RSCPublishing

ARTICLE

Identification and Discrimination of Binding Sites of an Organoruthenium Anticancer Complex to Single-Stranded Oligonucleotides by Mass Spectrometry

Suyan Liu, Kui Wu,* Wei Zheng, Yao Zhao, Qun Luo, Shaoxiang Xiong, Fuyi Wang*

Cite this: DOI: 10.1039/xoxxoooooox

Received 2014,
Accepted 2014

DOI: 10.1039/xoxxoooooox

www.rsc.org/

We herein report the identification of binding sites of an organometallic ruthenium anticancer complex [(η^6-biphenyl)Ru(en)Cl]$^+$ (**1**) to single-stranded oligodexylnucleotides (ODNs), 5′-$CCCA_4G_5C_6CC$-3′ (**I**) and 5′-$CCC_3G_4A_5CCC$-3′ (**II**), by mass spectrometry. The MS analysis of exonuclease ladders demonstrated that the 5′-exonuclease bovine spleen phosphodiesterase digestion of mono-ruthenated **I** and **II** by complex **1** was arrested solely at A_4 and partially at C_3 and G_4, respectively, and that the 3′-exonuclease snake venom phosphodiesterase digestion of the ruthenated ODNs was retarded solely at G_5 and G_4, respectively, due to the ruthenation. These results did not allow unambiguous identification of ruthenation sites on the metallated ODNs. In contrast, tandem mass spectrometry analysis with CID fragmentation of the mono-ruthenated ODNs provided sequential and complementary $[a_i - B]/w_i$ fragments, leading to unambiguous identification of G_5 in **I** and G_4 in **II** as the ruthenation sites on the ODN adducts, which is in line with the high selectivity of this complex towards guanine base as reported previously. These findings suggest that caution should be raised with regards to the identifications of binding sites of metal complexes, in particular ones with bulky ligands like biphenyl in complex **1**, to DNA by MS analysis of exonuclease ladders of the metallated adducts because the bulky ligands may take such an orientation that they block the exonuclease cleavage of 5′- or 3′-side the phosphodiester bonds adjacent to the binding sites, leading to digestion stalling at the nucleotides before the binding sites.

Introduction

Organometallic ruthenium complexes in the formula of [(η^6-arene)Ru(en)Cl]$^+$, where arene = benzene, *p*-cymene, biphenyl (**1**), dihydroanthrancene or tetrahydroanthrancene, etc. and en = ethylenediamine, are a family of promising anticancer drug candidates which are cytotoxic both *in vitro* and *in vivo*, even active against cisplatin-resistant cancer cells.[1, 2] As for cisplatin,[3] which is one of the mostly used anticancer drugs, DNA is thought to be a potential target for the Ru^{II} arene complexes[4-7] which preferentially bind to N7 of guanosine but have low affinity to N3 of thymidine and little affinity to N3 of cytidine and adenosine.[5] A great number of reports have demonstrated that the binding sites of cisplatin to DNA and the structural alternation of DNA duplex upon such bindings play a crucial role in the mechanism of action of the metallodrug.[3] Therefore the exact localization of DNA metallation by metal-based anticancer drugs/candidates and the structural consequence of the DNA metallation have attracted increasing attention.

Cisplatin has been demonstrated to bind to guanine selectively, forming 1,2-G,G-intrastranded crosslinked DNA adducts which account for about 65% of the total platinated DNA products.[3, 8] However, it has been shown that the bulky intercalator unit 1-[2-(acridin-9-ylamino)ethyl]-1,3-dimethylthiourea) (ACRAMTU-S) in an analog of cisplatin, $[PtCl(en)(ACRAMTU\text{-}S)](NO_3)_2$, could alter the binding-site specificity of Pt^{II}, leading to formation of more A-bound adducts which renders this complex a non-guanine specific platinum-based DNA modifier and accounting for the different biological activity of this mono-functional platinum complex.[9] The binding sites of ruthenium-based anticancer drug candidates KP1019, NAMI-A and RAPTA-T to different duplex oligonucleotides was also studied and compared with those of platinum-based chemotherapeutics such as cisplatin, carboplatin and oxaliplatin.[10] It has been showed that a strong preference for guanine bases was established irrespective of the sequence of oligonucleotide for these Ru(II)/Ru(III) complexes, perhaps responsive for the distinct mechanism of action of ruthenium-based anticancer complexes.[11, 12]

With the virtues of high sensitivity, low sample consumption and chemical specificity, electrospray ionisation mass spectrometry (ESI-MS) has become one of the most powerful tools for characterizing the diverse interactions, in particular elucidating the interaction sites of metal complexes with DNA.[13-15] Generally, there are two types of complementary mass spectrometric approaches for such work: MS analysis of the exonuclease ladders of DNA adducts and

MS/MS analysis of DNA adducts. The former one, also termed as ladder sequencing MS, involves in digestions of metallated DNA adducts by exonuclease, followed by MS or LC-MS analysis.[16-18] While in the latter approach, also termed as top-down MS, the DNA adducts were directly introduced into mass spectrometer and fragmentated under various excitation techniques.[19, 20] These two methods have been successfully applied to study the interactions of diverse metal complexes with DNA.[9, 10, 18-21] We have recently demonstrated that the combination of the two MS approaches are even more powerful in identifying the binding sites of ruthenium arene anticancer complexes to single-stranded oligodeoxynucleotides (ODNs) and found the novel thymine binding sites.[17]

It has been previously shown that the exonuclease digestions could be arrested at the sites where metal complexes such as platinum[22] and ruthenium[1, 17, 18] anticancer complexes coordinated to DNA bases, or chemical carcinogens such as polycyclic aromatic hydrocarbons (PAH)[23, 24] and 4 - (methylnitrosamino) - 1 - (3 - pyridyl) - 1 - butanone (NNK)[25] covalently bound to DNA bases. This provides structural information for localization of the binding/modification sites on DNA. However, when we recently studied the interaction between a ruthenium arene anticancer complex $[(\eta^6\text{-biphenyl})Ru(en)Cl]^+$ (**1**) and a 22-mer human telomeric ODN 5′-$A_1G_2G_3G_4(TTAGGG)_3$) by LC-MS, we observed arresting of the 5′-exonuclease digestion of the ruthenated adduct at A_{13} and A_{19}.[26] These seem to suggest that adenine base in DNA is also a binding site for complex **1**, inconsistent with previous reports, where complex **1** was showed to bind selectively to guanine base, being highly discriminatory between G and A bases.[5, 7] To address this controversial issue, in the present work, two short single-stranded ODNs, 5′-$CCCA_4G_5CCC$-3′ (**I**) and 5′-$CCC_3G_4A_5CCC$-3′ (**II**), were synthesised and reacted with complex **1**, and the ruthenated adducts were then characterised by ladder-sequencing and top-down MS analysis. The results demonstrated that the guanine bases in both ODN strands are the selective binding sites for complex **1**, but the biphenyl ligand of the G-bound **1** orient over the 5′-side, leading to arresting of 5′-exonuclease cleavage at the 5′-side nucleotides before the binding sites.

Materials and methods

Chemicals

$[(\eta^6\text{-biphenyl})Ru(en)Cl][PF_6]$ (**1**$[PF_6]$; en = ethylenediamine) was synthesized as described in the literature.[1] HPLC-purified oligodeoxynucleotides (ODNs) 5′-$CCCA_4G_5CCC$-3′ (**I**) and 5′-$CCCG_4A_5CCC$-3′ (**II**) were obtained as sodium salts from TaKaRa (Dalian, China), and the concentrations were determined by UV spectroscopy at 260 nm. Acetonitrile (HPLC grade) were purchased from Merck (Germany) and triethylammonium acetate buffer (TEAA, 1 M) from AppliChem (Germany). Bovine spleen phosphodiesterase (BSP) was bought from Sigma and snake venom phosphodiesterase (SVP) from Orientoxin (Shandong, China). The dialysis bag (1 kDa) was purchased from Viskase (USA). Aqueous solutions were prepared using MilliQ water (MilliQ Reagent Water System).

Sample preparation

The stock solutions of complex **1** (0.5 mM) and ODNs (1 mM) were prepared by dissolving the complex and ODNs, respectively, in deionised water, and then diluted as required prior to use.

To identify the binding sites of complex **1** on ODNs, the mixture of complex **1** with each ODN (molar ratio [Ru]/[ODN] = 0.2) incubated at 310 K for 24 h was dialysed against deionised water for 12 h to remove the unbound ruthenium complex. After freeze-dried, the samples were re-dissolved in 20 μL water, and partially digested by BSP or SVP. The digestions were carried out at 310 K with 0.8 μL (16 mU) of SVP in 10 mM Tris buffer containing 20 mM $MgSO_4$ (pH 8.8), or with 2.8 μL (28 mU) of BSP in 20 mM NH_4Ac buffer (pH 6.7), and then analysed by HPLC-ESI/MS.

High performance liquid chromatography (HPLC)

An Agilent 1200 series quaternary pump and a Rheodyne sample injector with a 20 μL loop, an Agilent 1200 series UV-Vis DAD detector and Chemstation data processing system were used. The mobile phases were water containing 20 mM TEAA (solvent A) and acetonitrile containing 20 mM TEAA (solvent B). The separation of the digests was carried out by using a C18 reversed-phase column (2.0 × 100 mm, Varian, Inc.) with a flow rate of 0.2 mL min^{-1}. The gradient was as follows (B): 1% from 0 to 5 min, 1% to 20% from 5 to 30 min, 20% to 80% from 30 to 32 min, 80% from 32 to 37 min, and resetting to 1% at 37 min. For the online HPLC-ESI-MS assays, a splitting ratio of 2/5 was used to introduce eluents into the mass spectrometer (Micromass Q-TOF, Waters).

Electrospray ionisation mass spectrometry (ESI-MS)

Negative ESI-MS spectra were obtained with a Micromass Q-TOF mass spectrometer (Waters) equipped with a Masslynx (ver 4.0) data processing system for analysis and post processing. The spray and cone voltages were 3.3 kV and 35 V, respectively. The collision energy was set up to 5 eV. The desolvation temperature was 353 K and the source temperature 413 K. Nitrogen was used as both cone gas and desolvation gas with a flow rate of 50 L h^{-1} and 500 L h^{-1}, respectively. The spectra were acquired in the range of *m/z* 200 ~ 2000. The mass accuracy of all measurements was within 0.01 *m/z* unit, and all *m/z* data are the mass-to-charge ratios of the most abundant isotopomer for the observed ions. For ESI-MS/MS analysis, $[M - 3H]^{3-}$ was selected as the parent ions for collision induced dissociation and the collision energies were set at the range of 16 to 22 eV, and the spectra were acquired in the range of *m/z* 200 ~ 2000.

Docking Analysis

The binding models were constructed using Sybyl X 1.1 program (Tripos Inc.), running on Dual-core Intel(R) E5300 CPU 2.60 GHz, RAM Memory 2 GB under the Windows XP system. Docking of the Ru complex onto G-N7 of ODNs **I** and **II** was achieved by manual independent manipulation according to procedures reported previously.[7] In brief, the crystal structure of complex **1** (CCDC 170362)[1] was manually adjusted to coordinate to G-N7 on ODNs **I** or **II** to match that of the crystallised (biphenyl)Ru-(Guo-N7) complexes.[4] A pseudo single bond between Ru centre and the centroid of the η^6-six-membered aromatic ring of biphenyl was built to provide a rotatable bond around which the biphenyl moiety could be manipulated, and the entire Ru ligand could be rotated independently of the DNA structure. Then the Gasteiger-

Huckel charges was added to the ODN complexes and they were energy-minimized using the Tripos force field with a distance-dependent dielectric and Powell gradient algorithm with an energy convergence value of 0.05 kcal·mol^{-1}.

Results and discussion

Firstly, the reaction mixture of complex **1** and ODN **I** at a molar ratio of [**1**]/[**I**] = 0.2, where the low molar ratio was applied to maintain the binding specificity, was analysed by LC-ESI-MS, which showed that the reaction produced only a mono-ruthenated adduct (Figure S1 in the Electronic supplementary information). Then, the dialysed reaction mixture was partially digested by 5′-exonuclease BSP, followed by LC-MS analysis of the exonuclease ladders. As shown in Figure 1a, two ruthenated ladders were observed at *m/z* 879.66 and 890.65, respectively, which correspond to mono-ruthenated ladder $[F_4'+\mathbf{1}']^{2-}$ (calculated (calc.) *m/z* 879.66) and its sodium adduct $\{[F_4'+\mathbf{1}']+Na^+\}^{2-}$ (calc. *m/z* 890.65) (Figure S2), respectively, where F_4' = 5′-A_4G_5CCC-3′ and **1**′ = [(η^6-bip)Ru(en)]$^{2+}$. The sodium ion added to the ODN fragment raised from the synthetic ODN which was provided as sodium salt. These results indicated that the BSP digestion was retarded at the adenine base (A_4) in the mono-ruthenated **I**, similar to that occurred in the BSP digestion of the ruthenated 22-mer human telomeric ODN 5′-$A_1G_2G_3G_4(TTAGGG)_3$.[26] No resistance at A_4 to BSP digestion was observed for free ODN **I** (data not shown), thus the arrest at A_4 is attributed to the binding of complex **1** to either A_4 or G_5 because the binding at A_4 or G_5 may prevent the phosphodiester bond between A_4 and G_5 from cleaving by BSP as did the covalent modification of ODNs by PHAs.[22, 24, 27, 28]

To complement the identification of the binding sites of complex **1** on **I**, 3′-exonuclease SVP was also applied to digest the aforementioned mono-ruthenated **I**. Two negative ions containing characteristic ruthenium isotopes (Figure 1b) were observed which are assignable to doubly-charged ladders $[F_5+\mathbf{1}']$ (observed (obs.) *m/z* 879.66, calc. *m/z* 879.66) and $\{[F_5+\mathbf{1}']+Na^+\}$ (obs. *m/z* 890.65, calc. *m/z* 890.65), respectively, where F_5 = 5′-$CCCA_4G_5$-3′ (Figure S3). This suggests that complex **1** probably bound to either G_5 or A_4, leading to missing of SVP digestion of the phosphodiester bond between G_5 and A_4. However, neither MS analysis of 5′-exonuclease BSP ladders nor MS analysis of 3′-exonuclease SVP ladders can allow unambiguous localization of the binding site of complex **1** on the mono-ruthenated **I**.

To further verify the effectiveness of exonuclease digestion for characterisation of binding sites of ruthenium arene complexes on ODNs, single-stranded ODN **II** (5′-$CCCG_4A_5CCC$-3′), an analogue of ODN **I** with only variation at the order of G and A bases was also synthesised and reacted with complex **1** at [**1**]/[**II**] = 0.2. The formation of mono-ruthenated **II** was confirmed by LC-MS (Figure S4). Then, the mono-ruthenated ODN **II** was digested by BSP and SVP, respectively, followed by LC-MS analysis of the exonuclease ladders. The results (Figure 2a) showed that two mono-ruthenated ladders $[F_3'+\mathbf{1}']$ (obs. *m/z* 1024.19, calc. *m/z* 1024.18) and $[F_4'+\mathbf{1}']$ (obs. *m/z* 879.66, calc. *m/z* 879.66), where F_3' = 5′-$C_3G_4A_5CCC$-3′ and F_4' = 5′-G_4A_5CCC-3′, and their sodium adducts were detected in the BSP digest (Figure S5), and that only one ruthenium-containing ladder $[F_4+\mathbf{1}']$

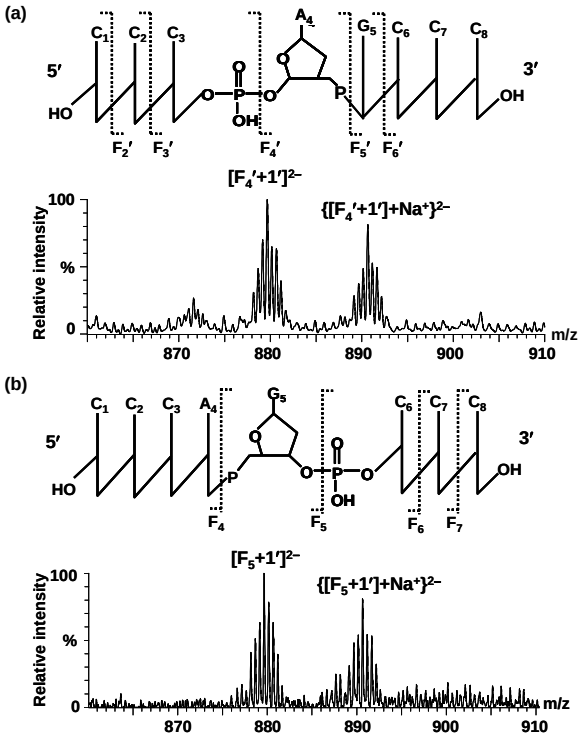

Figure 1. Schematic representations of BSP (a, top) and SVP (b, top) digestions of ODN **I** and corresponding mass spectra of BSP (a, bottom) and SVP (b, bottom) ladders of mono-ruthenated **I** by complex **1**. F_i' indicates the 3′-side ladders, F_i the 5′-side ladders; **1′** = [(η^6-bip)Ru(en)]$^{2+}$.

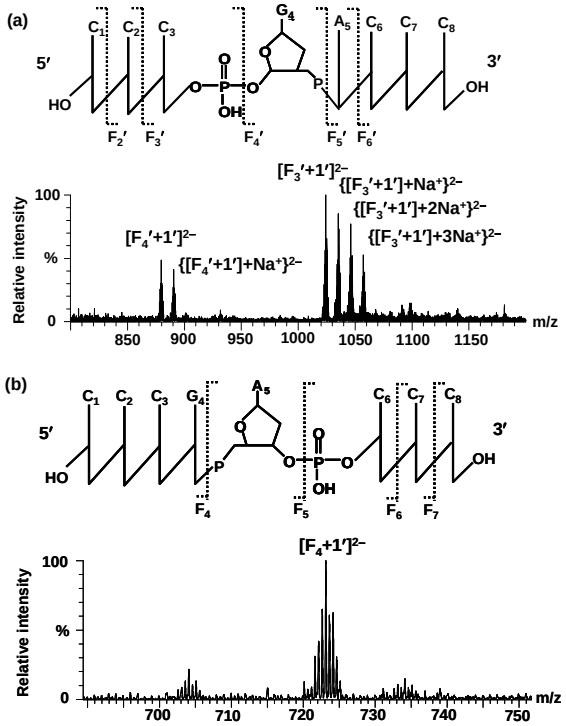

Figure 2. Schematic representations of BSP (a, top) and SVP (b, top) digestions of ODN **II** and corresponding mass spectra of BSP (a, bottom) and SVP (b, bottom) ladders of mono-ruthenated **II** by complex **1**. F_i' indicates the 3′-side ladders, F_i the 5′-side ladders; **1′** = [(η^6-bip)Ru(en)]$^{2+}$.

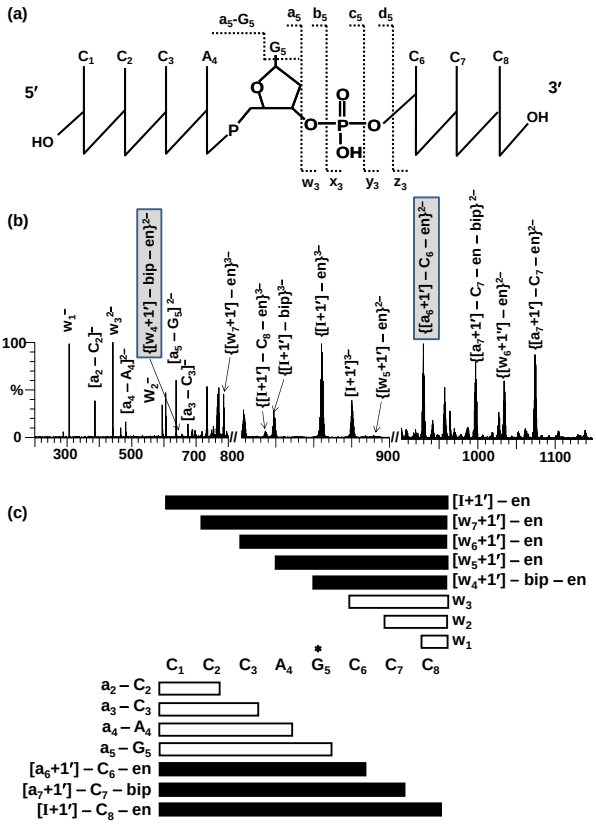

Figure 3. (a) Schematic diagram of MS/MS fragmentation of single-stranded ODN **I**; (b) MS/MS spectrum in the *m/z* range of 200 - 1150 for parent ion $[\mathbf{I}+\mathbf{1}']^{3-}$; (c) Diagrammatic illustration of the localisation of the binding site for ruthenium complex **1** on single-stranded ODN **I** based on the sequential and complementary $[a_i - B_i]/w_i$ fragments. **1′**: $[(\eta^6\text{-bip})Ru(en)]^{2+}$; blank box: unruthenated fragments w_i or $[a_i - B_i]$; filled box: mono-ruthenated fragments w_i or $[a_i - B_i]$; * indicates the ruthenation site deduced by the MS/MS results.

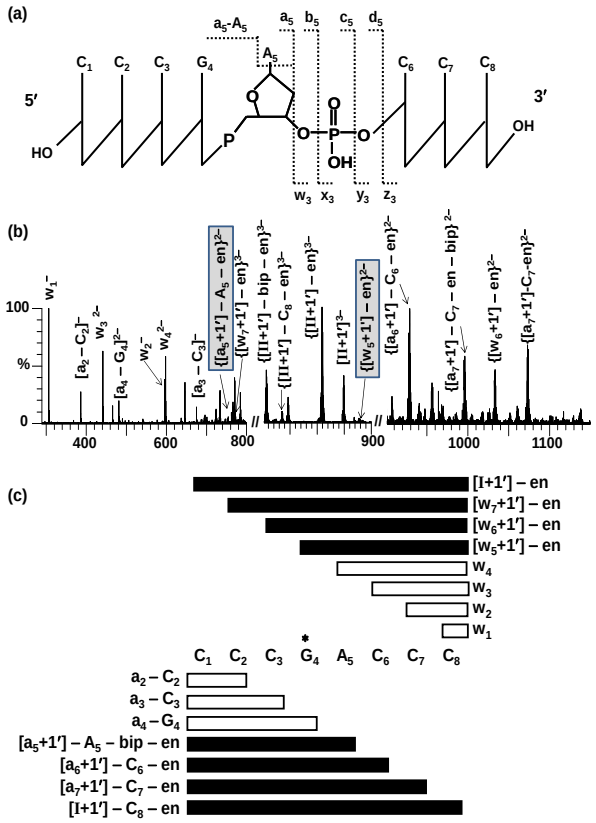

Figure 4. (a) Schematic diagram of MS/MS fragmentation of single-stranded ODN **II**; (b) MS/MS spectrum in the *m/z* range of 200 - 1150 for parent ion $[\mathbf{II}+\mathbf{1}']^{3-}$; (c) Diagrammatic illustration of the localization of the binding site for ruthenium complex **1** on **II** based on the sequential and complementary $[a_i - B_i]/w_i$ fragments. **1′** = $[(\eta^6\text{-bip})Ru(en)]^{2+}$; blank box: unruthenated fragments w_i or $[a_i - B_i]$; filled box: mono-ruthenated fragments w_i or $[a_i - B_i]$; * indicates the ruthenation site deduced by the MS/MS results.

(obs. *m/z* 723.13, calc. *m/z* 723.13; F_4 = 5′-CCC**G**$_4$-3′) was detected from the SVP ladders (Figure 2b and Figure S6). These results suggest that complex **1** may bind to either C_3 or G_4 in **II**. Again, by interpreting the MS data of the BSP and SVP ladders, we cannot conclude whether complex **1** binds at C_3 or G_4 in the mono-ruthenated **II**.

To achieve the unambiguous identification of the binding sites of complex **1** to ODNs **I** and **II**, tandem mass spectrometric analysis using collision induced dissociation (CID) was applied. During CID procedure, ODNs typically undergo the loss of a nucleobase B (one of the nucleobases A, C, G, or T) and a second elimination reaction leading to formation of a furan ring system may be followed by cleavage of the adjacent 3′-C-O phosphodiester bond of the deoxyribose, which yields sequential and complementary $[a_i - B_i]$ and w_i ions (Figure 3a).[29, 30] Cleavages at other locations along the phosphodiester linkage of DNA strand are significantly less abundant, which greatly simplifies spectral interpretation.[18, 31] The reaction mixtures of complex **1** and ODN **I** or **II** at a molar ratio of [**1**]/[ODNs] = 0.2 incubated at 310 K for 24 h were directly introduced into mass spectrometer and $[M - 3H]^{3-}$ was selected as the parent ions for CID fragmentation. According to the MS/MS spectrum of the mono-ruthenated **I**, no ruthenated w_i fragments from 3′-terminus up to w_3 were detected, while both unruthenated and ruthenated w_4 fragments were observed at *m/z* 606.09 (calc. *m/z* 606.09 for w_4^{2-}) and 656.04 (calc. *m/z* 656.04 for $\{[w_4+\mathbf{1}'] - bip - en\}^{2-}$), respectively, accompanied by the detection of larger mono-ruthenated fragments w_5, w_6, and w_7 with losing en or both bip and en ligands in complex **1** (Figure 3b, Figure S7 and Table S1). Meanwhile, the 5′-terminus $[a_i - B_i]$ fragments up to $[a_5 - G_5]$ were detected to be Ru-free, whereas mono-ruthenated fragment $[a_6 - C_6]$ was observed at *m/z* 929.61 (calc. *m/z* 929.62 for $\{[a_6+\mathbf{1}'] - C_6 - en\}^{2-}$), accompanied by the detection of larger mono-ruthenated $[a_7 - C_7]$ and $[\mathbf{I} - C_8]$ fragments. These complementary $[a_i - B_i]/w_i$ fragments (Figure 3c) allow unambiguous identification of G_5 in **I** as the sole binding site for complex **1**.

The binding sites of complex **1** on strand **II** were analogically identified by ESI-MS/MS, and the results are shown in Figure 4 and Table S2. From 3′-terminus until w_4, no ruthenated fragments were detected. Then both unruthenated and ruthenated fragments w_5^{2-} were observed at *m/z* 762.60 (calc. *m/z* 762.62 for w_5^{2-}) and 889.58 (calc. *m/z* 889.61 for $\{[w_5+\mathbf{1}'] - en\}^{2-}$), respectively. Larger mono-ruthenated w_i fragments with losing en or both bip and en ligands were also detected (Figures 4 and S8). Furthermore, for 5′-terminus $[a_i - B_i]$ fragments, $[a_2 - C_2]^-$, $[a_3 - C_3]^-$ and $[a_4 - G_4]^{2-}$ were only detected in Ru-free forms, while mono-ruthenated $[a_5 - A_5]^{2-}$, $[a_6 - C_6]^{2-}$ and $[a_7 - C_7]^{2-}$ losing en or both bip and en ligands were observed (Figures 4 and S8). These results revealed that G_4 on **II** was the binding site of complex **1**, in line with the high selectivity of this complex towards G reported in the literature.[5]

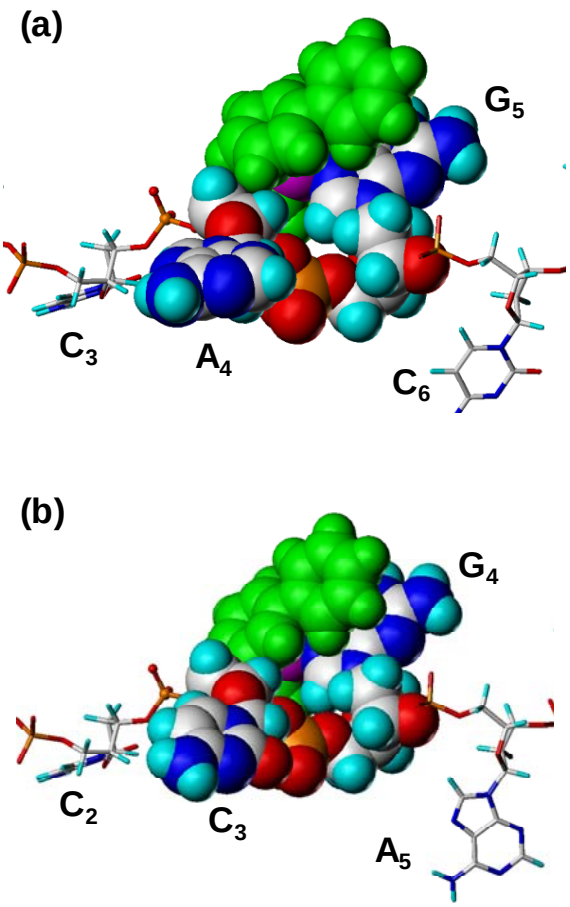

Figure 5. The molecular models of (a) ruthenated **I** by complex **1** at G_5-N7 and (b) ruthenated **II** at G_4-N7. Color code: biphenyl, green; Ru, purple; carbon, gray; oxygen, red; nitrogen, blue; hydrogen, light blue; phosphorus, yellow.

Combined with NMR studies, molecular modeling has previously demonstrated that a ruthenated ODN duplex, 5′-ATACATG$_7$G$_8$TACATA-3′·5′-TATG$_{18}$TACCATG$_{25}$TAT-3′, by complex **1** at G_{18} present two conformations, of which one has the pendant arene ring of biphenyl ligand in complex **1** intercalating between G_{18} and T_{17}, another has the biphenyl ligand orienting over the phosphodiester bond between T_{17} and G_{18}.[7] Thus, we speculate that a similar 5′-side orientation over the phosphodiester bond between the ruthenation sites and the 5′-side adjacent bases might occur when complex **1** binds to the single-stranded ODNs **I** at G_5 and **II** at G_4. As shown in Figure 5a, our molecular modeling indicates that when complex **1** binds to G_5 on strand **I**, the biphenyl ligand of complex **1** indeed orients over the phsophodiester bond between G_5 and A_4, which might account for the arrests of 5′-exonuclease BSP digestion at A_4 and 3′-exonuclease SVP digestion at G_5. The similar 5′-side orientation upon the binding of complex **1** at G_4 in ODN **II** is also observed in the molecular model of the ruthenated **II** by complex **1** (Figure 5b), perhaps being responsible for the arrests of BSP digestion at C_3 and SVP digestion at G_4. Such arresting of exonuclease digestion at 5′-side nucleotides adjacent to platinated guanosine is rarely happened to platinated DNA by cisplatin.[22]

It is notable that the single aromatic ring in cytosine is smaller in size than the double aromatic ring in adenine base so that the interactions, e.g. π-π stacking, between cytosine and the biphenyl ligand of complex **1**[4, 7] may be not as efficient as those between adenine and biphenyl to block the cleavage of the phosphodiester bond between C_3 and G_4 when complex **1** bind to ODN **II** at G_4. Thus, the 5′-exonuclease BSP digestion of the ruthenated **II** by complex **1** at G_4 was found to be arrested partially at both C_3 and G_4.

The similar resistance to exonuclease digestion resulting from covalent binding of bulky polycyclic aromatic hydrocarbon (PAHs) derivatives to single-stranded oligonucleotides has been reported previously.[24, 27, 28, 32] The chiral diol epoxide isomers 7β,8α-dihydroxy-9α,10α-epoxy-7,8,9,l0-tetrahydrobenzo[*a*]pyrene[(+)-*anti*-BPDE)] and 7α,8β-dihydroxy-9β,10β-epoxy-7,8,9,10-tetrahydrobenzo[*a*]pyrene[(−)-*anti*-BPDE)], which are carcinogenic metabolites of PAHs, reacted with single-stranded ODNs to form a pair of diastereomeric dG adducts *via* ring opening at the reactive benzylic position.[23, 24, 25] The hydrocarbon portion of the (−)-*trans*-*anti*-BPDE at dG adducts orients towards the 3′-end, stalling the SVP hydrolysis of 3′-side phosphodiester adjacent to the modification site, whereas the bulky PAH ring in (+)-*trans*-*anti*-BPDE at dG adducts lies towards the 5′-end, inhibiting the spleen phosphodiesterase (SPD) cleavage of the 5′-side phosphodiester bond of the modified guanine site.[28] The adenine-modified oligonucleotides (dA adducts) with benz[*a*]anthracene and benzo[*c*]phenanthrene diol epoxides also showed diastereomer-dependent stalling for both SVP and SPD digestion.[32] However, the patterns of resistance to exonuclease digestion of the dA adducts are different from those of dG adducts. The SVP hydrolysis of both *R*- and *S*-adducts at dA was blocked at the 5′-side phosphodiester bond adjacent to the modified adenine base, and then jumped to the 5′-side phosphdiester bond adjacent to the N(−1) nucleotide, producing a dinucleotide adduct dN(−1)dA, while the SPD cleavage of the 5′-side phosphdiester bond adjacent to the modified adenine base by *R*- or *S*-PAHs was found to be retarded.[32]

For MS/MS analysis, the dissociation of phosphodiester bonds in the backbone of ODNs occurs in gas phase, and the ruthenium complex **1** with the bulky biphenyl ligand binding to guanine base in ODNs **I** and **II** has little steric effect on the fragmentation of the phosphate backbones. Therefore, the fragmentation of the ruthenated strands **I** and **II** was similar to that of non-modified ODN strands, and the resulting sequential and complementary fragments provide sufficient structural information for discrimination of the binding sites of the ruthenium complex on ODN strands (Figures 3 and 4).

Conclusions

In the present work, our mass spectrometric studies showed that the reactions of the ruthenium anticancer complex [(η^6-biphenyl)Ru(en)Cl]$^+$ (**1**) with single-stranded oligonucleotides (ODNs), 5′-CCCA$_4$G$_5$C$_6$CC-3′ (**I**) and 5′-CCC$_3$G$_4$A$_5$CCC-3′ (**II**), at a low molar ratio of [**1**]/[ODN] afforded two mono-ruthenated ODN adducts. The bulky arene ligand in complex **1** appears to orient towards the 5′-side of the ruthenation sites *via* interactions with adjacent bases, blocking the 5′- and 3′-exonuclease hydrolysis of the 5′-side phsophodiester bonds adjacent to the ruthenated guanosine and leading to formation of ruthenated 5′-NG~ and ~NG-3′ ladders, respectively. These results cannot allow unambiguous identification of the binding sites of complex **1** on the ODN adducts. In contrast, due to little effect on the gaseous dissociation of phosphodiester bonds of ODNs arising from the ruthenation, tandem mass spectrometry

analysis of the ruthenated ODN adducts provided sequential and complementary fragments, clearly indicating that complex **1** selectively bound to G_5 in **I** and G_4 in **II**. These findings imply that much attention should be paid to the steric effects of bulky ligands in metal complexes on the exonuclease digestion, which may interfere with the correct identification of metallation sites on DNA by MS analysis of exonuclease ladders of the metallated DNA adducts.

Acknowledgements

We thank NSFC (Grant Nos. 21135006, 21127901, 21275148 and 21321003), the 973 Program of MOST (2013CB531805) and the Innovation Method Fund of China (2012IM030400) for support, and Professor Peter J. Sadler of the University of Warwick for stimulating discussion.

Notes

[a] Beijing National Laboratory for Molecular Sciences, CAS Key Laboratory of Analytical Chemistry for Living Biosystems, Beijing Centre for Mass Spectrometry, Institute of Chemistry, Chinese Academy of Sciences, Beijing 100190, PR China. E-mail: fuyi.wang@iccas.ac.cn, wukui@iccas.ac.cn.

† Electronic Supplementary Information (ESI) available: MS(/MS) (Tables S1 - S2, Figures S1 - S8). See DOI: 10.1039/b000000x/

References

1. R. E. Morris, R. E. Aird, P. D. Murdoch, H. M. Chen, J. Cummings, N. D. Hughes, S. Parsons, A. Parkin, G. Boyd, D. I. Jodrell and P. J. Sadler, *J. Med. Chem.*, 2001, **44**, 3616-3621.
2. R. E. Aird, J. Cummings, A. A. Ritchie, M. Muir, R. E. Morris, H. Chen, P. J. Sadler and D. I. Jodrell, *Br. J. Cancer*, 2002, **86**, 1652-1657.
3. E. R. Jamieson and S. J. Lippard, *Chem. Rev.*, 1999, **99**, 2467-2498.
4. H. M. Chen, J. A. Parkinson, S. Parsons, R. A. Coxall, R. O. Gould and P. J. Sadler, *J. Am. Chem. Soc.*, 2002, **124**, 3064-3082.
5. H. M. Chen, J. A. Parkinson, R. E. Morris and P. J. Sadler, *J. Am. Chem. Soc.*, 2003, **125**, 173-186.
6. Y. K. Yan, M. Melchart, A. Habtemariam and P. J. Sadler, *Chem. Commun.*, 2005, 4764-4776.
7. H. K. Liu, S. J. Berners-Price, F. Y. Wang, J. A. Parkinson, J. J. Xu, J. Bella and P. J. Sadler, *Angew. Chem. Int. Ed.*, 2006, **45**, 8153-8156.
8. Y. W. Jung and S. J. Lippard, *Chem. Rev.*, 2007, **107**, 1387-1407.
9. C. G. Barry, H. Baruah and U. Bierbach, *J. Am. Chem. Soc.*, 2003, **125**, 9629-9637.
10. M. Groessl, Y. O. Tsybin, C. G. Hartinger, B. K. Keppler and P. J. Dyson, *J. Biol. Inorg. Chem.*, 2010, **15**, 677-688.
11. P. C. A. Bruijnincx and P. J. Sadler, *Curr. Opin. Chem. Biol.*, 2008, **12**, 197-206.
12. P. J. Dyson and G. Sava, *Dalton Trans.*, 2006, 1929-1933.
13. M. Petkovic and T. Kamceva, *Metallomics*, 2011, **3**, 550-565.
14. J. L. Beck, M. L. Colgrave, S. F. Ralph and M. M. Sheil, *Mass Spectrom. Rev.*, 2001, **20**, 61-87.
15. S. A. Hofstadler and R. H. Griffey, *Chem. Rev.*, 2001, **101**, 377-390.
16. N. Tretyakova, B. Matter, A. Ogdie, J. S. Wishnok and S. R. Tannenbaum, *Chem. Res. Toxicol.*, 2001, **14**, 1058-1070.
17. K. Wu, W. B. Hu, Q. Luo, X. C. Li, S. X. Xiong, P. J. Sadler and F. Y. Wang, *J. Am. Soc. Mass Spectrom.*, 2013, **24**, 410-420.
18. K. Wu, Q. Luo, W. B. Hu, X. C. Li, F. Y. Wang, S. X. Xiong and P. J. Sadler, *Metallomics*, 2012, **4**, 139-148.
19. K. Breuker, M. Jin, X. M. Han, H. H. Jiang and F. W. McLafferty, *J. Am. Soc. Mass Spectrom.*, 2008, **19**, 1045-1053.
20. A. E. Egger, C. G. Hartinger, H. Ben Hamidane, Y. O. Tsybin, B. K. Keppler and P. J. Dyson, *Inorg. Chem.*, 2008, **47**, 10626-10633.
21. C. G. Hartinger, M. Groessl, S. M. Meier, A. Casini and P. J. Dyson, *Chem. Soc. Rev.*, 2013, **42**, 6186-6199.
22. F. Gonnet, F. Kocher, J. C. Blais, G. Bolbach, J. C. Tabet and J. C. Chottard, *J. Mass Spectrom.*, 1996, **31**, 802-809.
23. B. Wang, J. M. Sayer, H. Yagi, H. Frank, A. Seidel and D. M. Jerina, *J. Am. Chem. Soc.*, 2006, **128**, 10079-10084.
24. A. M. Cheh, H. Yagi and D. M. Jerina, *Chem. Res. Toxicol.*, 1990, **3**, 545-550.
25. S. Park, M. Seetharaman, A. Ogdie, D. Ferguson and N. Tretyakova, *Nucleic Acids Res.*, 2003, **31**, 1984-1994.
26. K. Wu, S. Y. Liu, Q. Luo, W. B. Hu, X. C. Li, F. Y. Wang, R. H. Zheng, J. Cui, P. J. Sadler, J. F. Xiang, Q. Shi and S. X. Xiong, *Inorg. Chem.*, 2013, **52**, 11332-11342.
27. P. Chary and R. S. Lloyd, *Chem. Res. Toxicol.*, 1996, **9**, 409-417.
28. B. Mao, B. Li, S. Amin, M. Cosman and N. E. Geacintov, *Biochemistry*, 1993, **32**, 11785-11793.
29. S. A. McLuckey, G. J. Vanberkel and G. L. Glish, *J. Am. Soc. Mass Spectrom.*, 1992, **3**, 60-70.
30. S. A. McLuckey and S. Habibigoudarzi, *J. Am. Chem. Soc.*, 1993, **115**, 12085-12095.
31. J. Wu and S. A. McLuckey, *Int. J. Mass spectrom.*, 2004, **237**, 197-241.
32. P. Ilankumaran, L. K. Pannell, P. Gebreselassie, A. S. Pilcher, H. Yagi, J. M. Sayer and D. M. Jerina, *Chem. Res. Toxicol.*, 2001, **14**, 1330-1338.

